http://www.ejchem.net

ISSN: 0973-4945; CODEN ECJHAO
E-Journal of Chemistry
2012, **9(4)**, 2429-2438

Synthesis and Characterisation of Penta-Bismuth Hepta-Oxide Nitrate, $Bi_5O_7NO_3$, as a New Adsorbent for Methyl Orange Removal from an Aqueous Solution

ESHRAQ AHMED ABDULLAH[1,*], ABDUL HALIM ABDULLAH[1,2], ZULKARNAIN ZAINAL[1,2], MOHD ZOBIR HUSSEIN[1,2], AND TAN KAR BAN[1]

[1]Department of Chemistry, Faculty of Science, Universiti Putra Malaysia, 43400 Serdang, Selangor, Malaysia
[2]Advanced Material and Nanotechnology Laboratory, Institute of Advanced Technology, Universiti Putra Malaysia, 43400 Serdang, Selangor, Malaysia

yemenahmed2009@gmail.com

Received 14 November 2011; Accepted 16 January 2012

Abstract: This paper presents the synthesis of penta-bismuth hepta-oxide nitrate, $Bi_5O_7NO_3$, via the chemical precipitation method. After calcination, the precipitate was characterised by several methods, which included X-ray powder diffraction, X-ray photoelectron spectroscopy, scanning and transmission electron microscopy, Fourier transform infrared, thermogravimetric analysis, BET surface area and pH drift method to determine the pH of point of zero charge (pH_{pzc}). The study results revealed that $Bi_5O_7NO_3$ had an orthorhombic crystal structure, a surface area of 1.6 m^2 g^{-1} and a point of zero charge at pH 9.7. The chemical state of $Bi_5O_7NO_3$ indicated the presence of three oxidation states of bismuth centre. Furthermore, the decolourization ability of $Bi_5O_7NO_3$ to remove the azo dye was also evaluated. Although it had lower surface area, the removal efficiency was extremely good. This finding suggests that $Bi_5O_7NO_3$ could be used as a promising adsorbent for azo dye removal. The XPS spectra showed that the accumulation of dye onto $Bi_5O_7NO_3$ could be due to the anion exchange process, suggesting the birth of a new anion exchanger for azo dye removal.

Keywords: Penta-bismuth hepta-oxide nitrate, new anion exchanger, X-ray photoelectron spectroscopy, methyl orange.

Introduction

Penta-bismuth hepta-oxide nitrate, $Bi_5O_7NO_3$, is a layered structure of bismuth oxide that belongs to the Bi_2O_3-N_2O_5 system[1]. The crystal structure consists of two layers of $^{2}_{\infty}[BiO]^{+}$ that are connected by the $^{1}_{\infty}[Bi_4O_8]^{4-}$ units. The $^{2}_{\infty}[BiO]^{+}$ layers and $^{1}_{\infty}[Bi_4O_8]^{4-}$ units form a framework structure, while the nitrate groups fill the channels in this structure[2].

The preparation of $Bi_5O_7NO_3$ by the thermal decomposition of basic bismuth nitrate and bismuth nitrate penta-hydrate has been reported by Kodama (1994)[1]. It is also produced as an intermediate compound in the early stages of thermal decomposition of poly-cationic $[Bi_6O_4(OH)_4](NO_3)_6$[3]. The characterisation of this compound, however, is limited to thermal analysis and x-ray diffraction pattern. Notably, reports on the use of $Bi_5O_7NO_3$ as an adsorbent are very scarce and limited to the removal and solidification of halogenides[1,4].

The objective of this study is to synthesize $Bi_5O_7NO_3$ via the precipitation method as a new pathway to produce this material for commercial yield. To gain good indicators on the correlation between the structural characteristics of $Bi_5O_7NO_3$ and its adsorptive performance, several analytical techniques were used. The adsorption ability of $Bi_5O_7NO_3$ was evaluated using the methyl orange (MO) dye as a model pollutant in an aqueous solution.

Materials and Methods

Materials

In order to synthesise penta-bismuth hepta-oxide nitrate, $Bi_5O_7NO_3$, bismuth nitrate penta-hydrate, $Bi(NO_3)_3.5H_2O$ (98%, Acros), nitric acid (65%, Fischer Scientific) and ammonium hydroxide (25%, Merck) were used. The adsorptive performance of the synthesised material to remove the methyl orange (MO) dye (Sigma-Aldrich) was compared to that of granular activated carbon, GAC, (KI6070, Kekwa Indah Sdn. Bhd.) and chitosan flakes (Sigma Aldrich) with a molecular weight of 200,000. GAC was ground, sieved to obtain a uniform size and oven-dried at 110°C for 24h. All chemicals were used as received, except for ammonium hydroxide, which was diluted to give a concentration of 50% v/v.

Synthesis of $Bi_5O_7NO_3$

Penta-bismuth hepta-oxide nitrate, $Bi_5O_7NO_3$, was synthesized by adding the ammonium hydroxide solution to a 20 ml concentrated nitric acid solution containing 10.0 g of $Bi(NO_3)_3.5H_2O$ with continuous stirring until pH 9 was obtained. The suspension was aged for 1h with vigorous stirring. The precipitate obtained was then filtered, washed with distilled water and oven-dried at 110°C overnight. The resulting powder was calcined in an open air horizontal tube furnace at 450°C for 1h.

Characterisation

The X-ray powder diffraction (XRD) pattern in the 2θ range of 10 - 70° was recorded using an X-Pert Pro PANalytical PW 3040 MPD (Philips) with CuKα radiation. The Fourier transform infrared spectra were recorded on a PerkinElmer Spectrum 100 series in the range of 4000 – 280 cm^{-1} under the attenuated total reflection (ATR) mode using a diamond module. Thermogravimetric analysis was performed using a TGA/SDTA 851 PerkinElmer thermal analyzer. The samples were heated in a stream of nitrogen gas flow of 50 ml min^{-1} with a heating rate of 2° min^{-1} up to 800°C. The textural characteristics of $Bi_5O_7NO_3$ including the surface area, pore volume and pore size distribution were determined using the N_2 adsorption-desorption technique. The N_2 adsorption-desorption isotherm of the synthesized $Bi_5O_7NO_3$ was measured at -196°C on a Quantachrome AS1Win™ version 2.0 sorptometer.

The pH at the point of zero charge (pH_{pzc}) of the $Bi_5O_7NO_3$ sample was determined by the drift equilibrium method reported by Rivera *et al.* [5,6]. The series samples of 50 cm^3 of NaCl (0.01 molar) as a background electrolyte were prepared. In addition, the initial pH of the electrolyte solution was adjusted to 2 – 12 by a small addition of HCl or NaOH solution. A certain amount of $Bi_5O_7NO_3$ (0.15 g) was added and the solution was shaken at a constant agitation speed in a water bath shaker for 48 h before the final pH was measured. The pH at which the curve crossed the line of $pH_{initial} = pH_{final}$ was taken as pH_{pzc}.

Microstructure characterisation was carried out using a LEO 912AB energy filter transmission electron microscope (TEM) and a TEOL TSM 6400 scanning electron microscope (SEM). Furthermore, the surface chemistry of the adsorbent was determined by an X-ray photoelectron spectroscopy (XPS). The XPS spectra were acquired at room temperature with an XPS AXIS ULTRA instrument using the Al-Kα (1486.6 eV) monochromatic radiation source. Diffuse reflectance spectra were recorded by using a PerkinElmer, Lambda 35 UV-Vis spectrometer.

Adsorption Studies

One gram of adsorbent was suspended in a 20 ppm, 1.0 L methyl orange dye solution. The suspension was magnetically stirred for 3 h at 25°C. After the pre-determined time intervals, 10 ml of the dye solution was withdrawn and filtered through a 0.45 μm filter. The dye concentration was determined spectrophotometrically at λ_{max} of 463 nm using a UV-1650 PC spectrophotometer (Shimadzu).

Results and Discussion

X-ray Powder Diffraction

Figure 1 shows the XRD profile of $Bi_5O_7NO_3$. Most of the diffraction lines could be indexed by a unit cell of an orthorhombic $Bi_5O_7NO_3$ (ICDD No. 00-051-0525). Some peaks belonging to the Bi_2O_3 monoclinic phase were discerned at 2θ = 23.17, 48.50, 59.8, 62.50 and 67.64º. Meanwhile, minute traces of the unclacined sample were also detected. The lattice constants of $Bi_5O_7NO_3$ were a = 16.28Å, b = 5.5480Å, and c = 23.3010Å. The particle size of the material estimated by using the Debye-Scherer equation was around 35.6 nm.

Fourier Transform Infrared Spectrum (FTIR)

The type of functional groups appeared on the $Bi_5O_7NO_3$ surface was clarified by using the FTIR spectrum, as illustrated in Figure 2. Strong absorption bands around 1300 and 1375 cm^{-1} can be assigned to the symmetric and asymmetric stretching modes of the coordinated NO_3^- group[7,8]. The absorption band at 1031 cm^{-1} indicated the presence of mono-dentate nitrate groups[9]. The strong absorption bands that appeared in the range of 300 – 800 cm^{-1} can be attributed to the stretching modes of the Bi-O bonds of $Bi_5O_7NO_3$. It appeared that these results were in close agreement with the reported data for bismuth oxide[10,11].

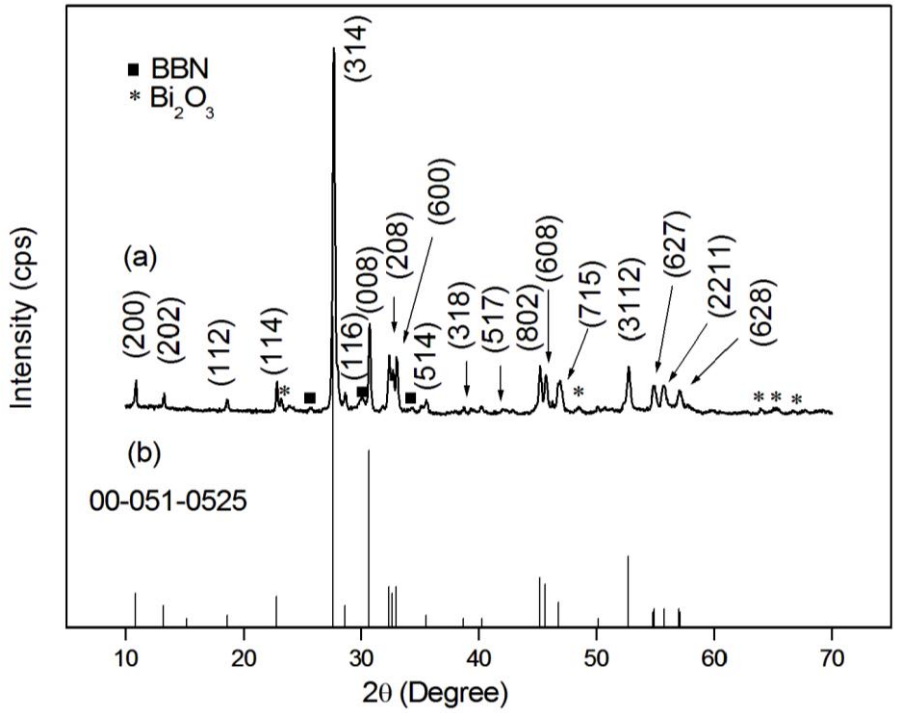

Figure 1. XRD pattern of $Bi_5O_7NO_3$ sample (a) and the ICDD 00-051-0525 is included for comparison (b).

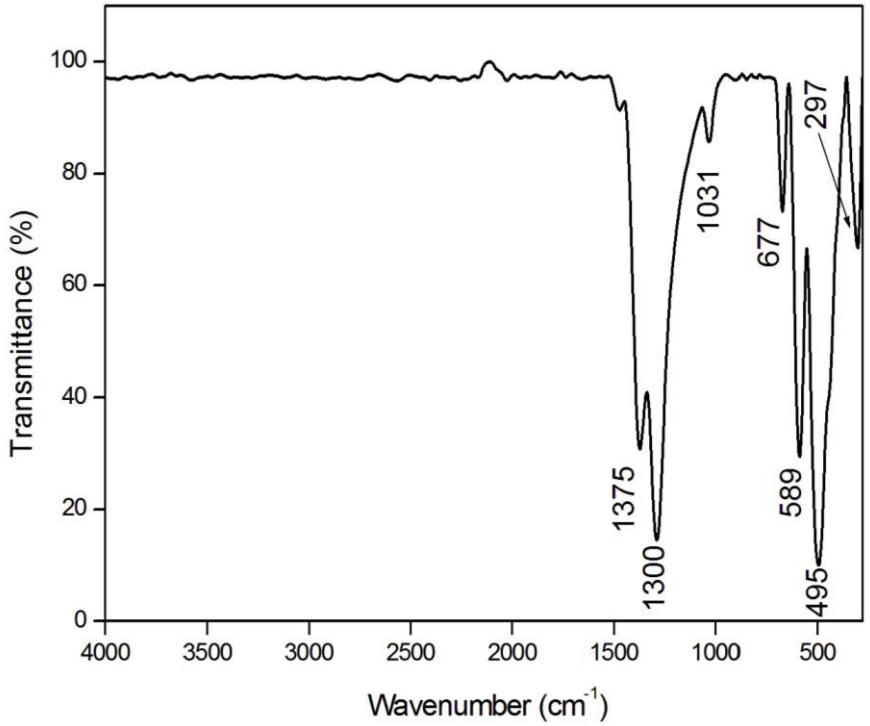

Figure 2. FTIR spectrum of $Bi_5O_7NO_3$.

Thermogravimetric Analysis

The thermal stability and decomposition products of $Bi_5O_7NO_3$ were evaluated by using the thermogravimetric analysis (TGA) (Figure 3). As shown in Figure 3, the thermal decomposition of $Bi_5O_7NO_3$ involved two steps of weight loss. The first weight loss of 3.2% observed around 460°C can be attributed to the release of the NO group, while the second weight loss of 1.0% at 545°C can be assigned to oxygen molecules. The total weight loss of 4.2% was comparable to the reported value of 4.4% observed from the decomposition of $Bi_5O_7NO_3$ to α-Bi_2O_3 at 600°C as suggested in Equation (1) below[1,3,12]:

$$Bi_5O_7NO_3 \rightarrow {}^{5}/_{2}\, Bi_2O_3 + NO + {}^{3}/_{4}\, O_2 \qquad (1)$$

X-ray Photoelectron Spectroscopy (XPS)

A unique application of any molecule is reflected by its physicochemical properties. Thus, the chemical environments of the elements detected on the $Bi_5O_7NO_3$ surface were analyzed using the XPS technique. The peak positions were corrected for the surface charge using C 1s peak at 284.5 eV as a reference. The typical spectrum (not shown) showed that Bi, O, N and C were the elements detected on the $Bi_5O_7NO_3$ surface. Figure 4a shows the 4f core electron spectrum of bismuth. The core level peaks located at the binding energies of 158.9 and 163.9 eV can be attributed to Bi $4f_{7/2}$ and Bi $4f_{5/2}$ orbitals of the bismuth centre, respectively. The shoulder observed at higher energy of Bi 4f might be assigned to the remaining bismuth basic nitrate impurities. The similarity of the binding energies of Bi 4f of $Bi_5O_7NO_3$ with that in Bi_2O_3 implying the three oxidation states of bismuth centre[13].

Figure 4b shows the deconvoluted XPS spectrum near the O 1s core level region for $Bi_5O_7NO_3$. The observed peaks showed a marked broadening towards higher binding energies indicating the presence of high content oxygen groups on the $Bi_5O_7NO_3$ surface. The peak at 529.7 eV coincided with the binding energy of O^{2-} of bismuth oxide[14,15], hence, this can be assigned to the binding energy of O^{2-} in $Bi_5O_7NO_3$. The O 1s peak around 531.0 eV was probably due to the existence of surface carbonate impurities, whereas the O 1s core level peak observed at 531.6 eV was due to the presence of nitrate groups NO_3^{-}[16].

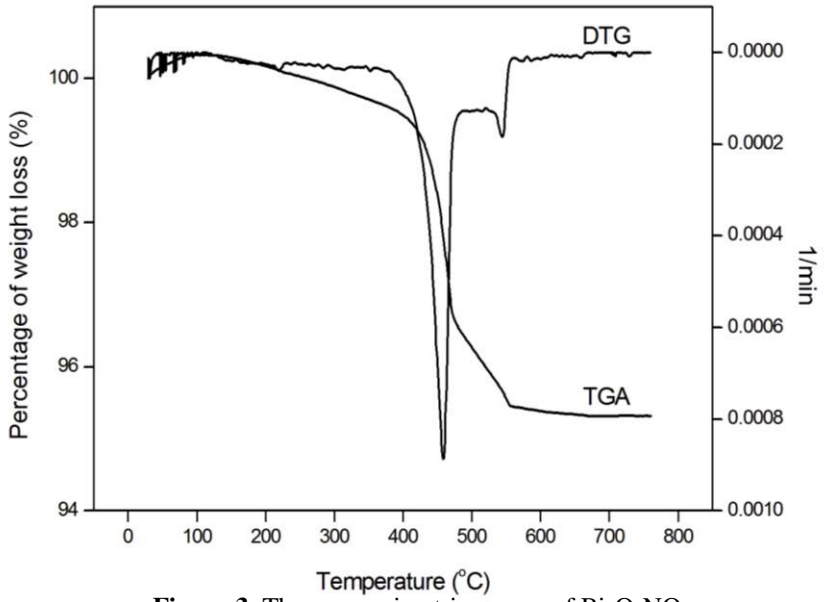

Figure 3. Thermogravimetric curves of $Bi_5O_7NO_3$.

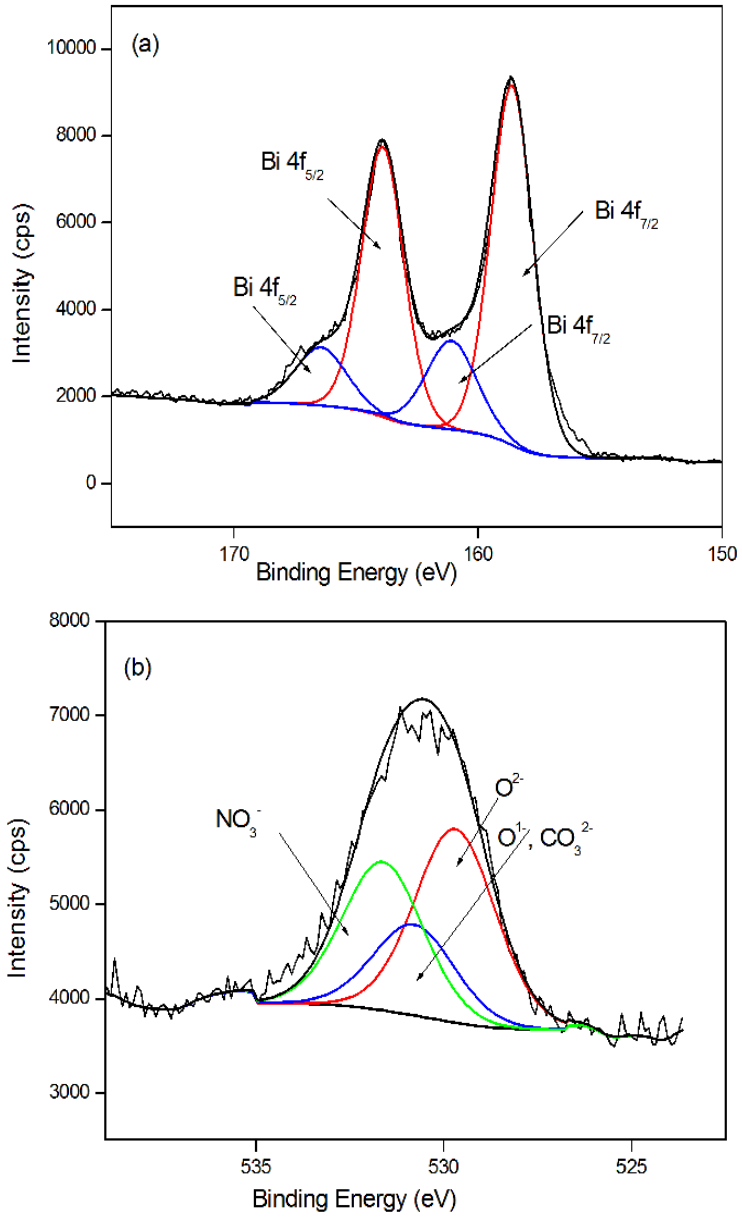

Figure 4. XPS results of (a) deconvoluted Bi 4f region and (b) O 1s region of $Bi_5O_7NO_3$.

Surface Area, Pore Size Distribution and Microstructure Features

Based on the IUPAC classification, the shape of the N_2 adsorption-desorption isotherm of $Bi_5O_7NO_3$ (Figure 5) belongs to type II isotherm, which implies the presence of certain amounts of macro- and mesopore walls in the sample[17]. The hysteresis loop of $Bi_5O_7NO_3$ was of type H3, which associates with plate-like particles giving rise to narrow slit-shaped pores[18]. The pore size distribution determined by the Barret-Joyner-Halenda (BJH) method can be observed in the inset of Figure 5.

It could be seen that the sample exhibited a pore size distribution in the mesopore and macropore domains implying bimodal distributions. The BET surface area, pore volume and radius of the adsorbent were found to be 1.6 $m^2 g^{-1}$, 0.033 $cm^3 g^{-1}$ and 17.14 Å, respectively.

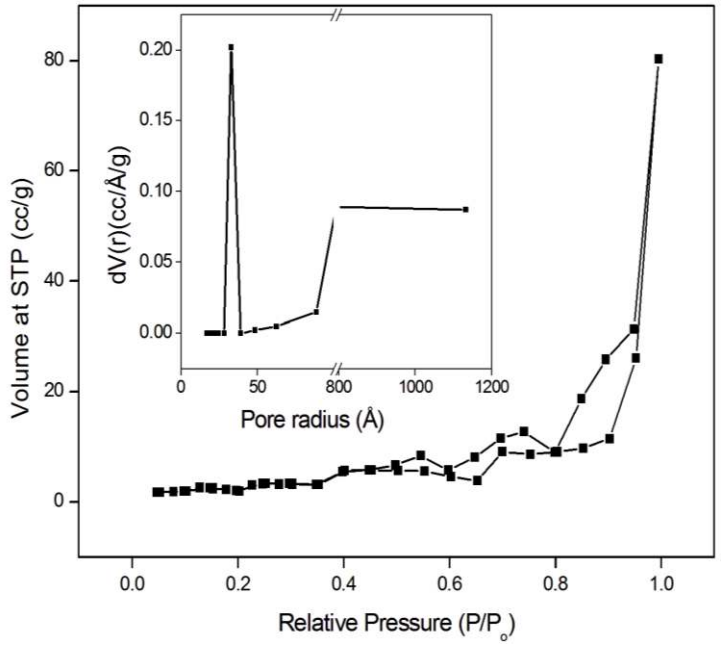

Figure 5. N_2 adsorption-desorption isotherm of $Bi_5O_7NO_3$ and pore size distribution.

On the other hand, the structural morphology of $Bi_5O_7NO_3$ was studied from the SEM and TEM images. The SEM image (Figure 6a) showed that the $Bi_5O_7NO_3$ surface consisted of highly aggregated plate-like particles, which were built from two-dimensional sheets with a smooth surface, as shown in the TEM image (Figure 6b).

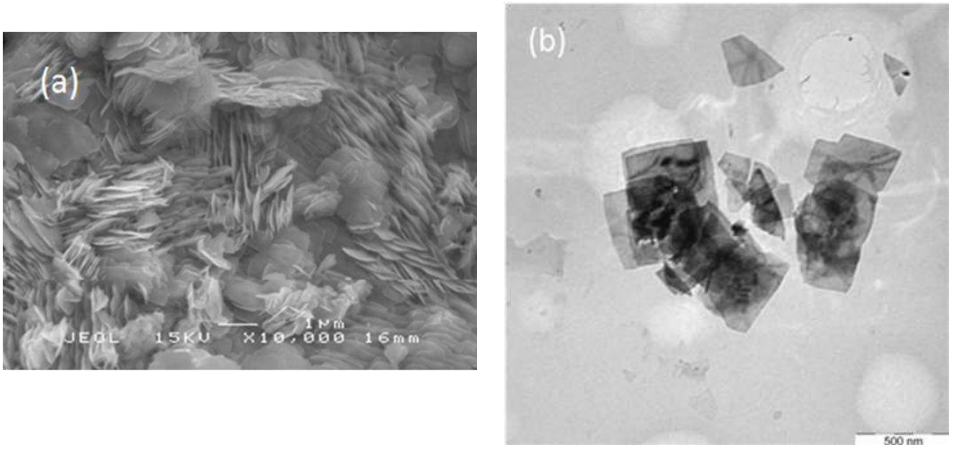

Figure 6: Microscopic observations (a) SEM and (b) TEM for $Bi_5O_7NO_3$, respectively.

pH of Point of Zero Charge (pH_{pzc})

The pH of point of zero charge is an important property of solid surface in aqueous solutions. It describes the ability of sorbent surface to accumulate adsorbate molecules. The pH_{pzc} of $Bi_5O_7NO_3$ assessed by the pH drift method was found to be 9.7 (Figure7), indicating that the positively charged surface occupied a wide range of pH.

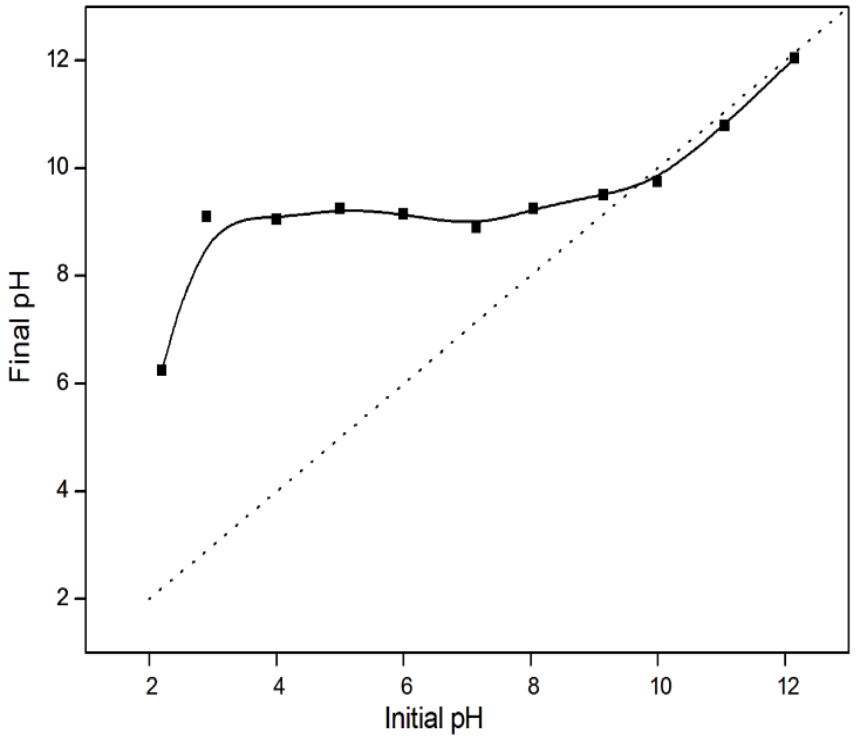

Figure 7: Determinations of pH_{pzc} of $Bi_5O_7NO_3$ by the pH drift method.

Adsorption Properties of $Bi_5O_7NO_3$

The adsorptive performance of the as-prepared $Bi_5O_7NO_3$ to remove methyl orange from the aqueous solution was investigated and compared to that of powdered activated carbon (PAC) and chitosan (Figure 8). Compared to activated carbon, the sorption capacity of $Bi_5O_7NO_3$ was significantly lower due to the large specific surface area of activated carbon. However, the adsorption efficiency or adsorption capacity per unit of the $Bi_5O_7NO_3$ surface area was sufficiently high. Furthermore, there was a significant difference in the sorption capacity compared to chitosan. This might be attributed to the structural characteristic effect, which produced a suitable removal environment for the anionic dye onto $Bi_5O_7NO_3$.

Since the ion exchange ability of $Bi_5O_7NO_3$ for iodine, chloride and bromide has been reported[1,4], it is interesting to see whether the removal of MO dye by $Bi_5O_7NO_3$ via adsorption is complemented by the ion exchange process. Thus, the ion exchange process was investigated by using the X-ray photoelectron spectroscopy study. The XPS spectra of $Bi_5O_7NO_3$ before and after the MO dye adsorption are shown in Figure 9. Before the adsorption, there was remarkable broadening towards higher binding energy of O 1s core level attributed to the presence of NO_3^- groups. After the MO dye adsorption, the broadening of the O 1s core level spectrum was not observed.

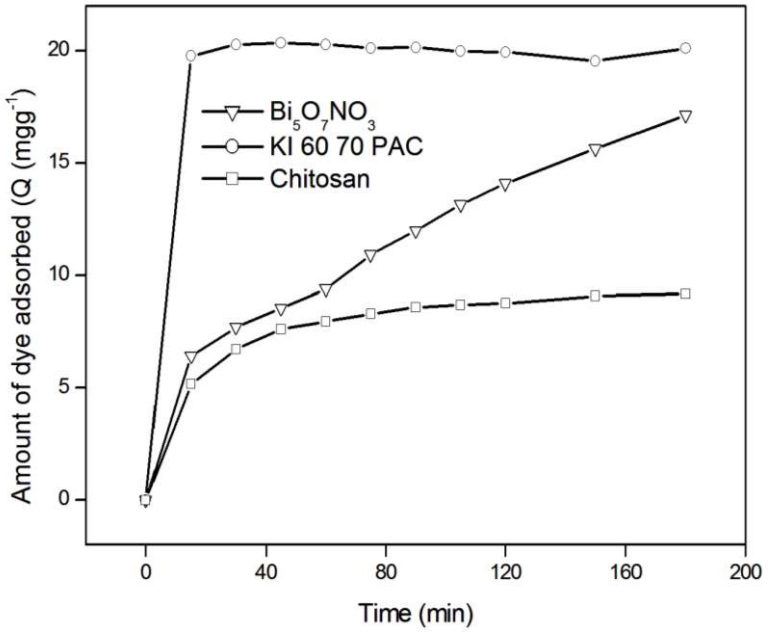

Figure 8: Preliminary evaluation of adsorptive performance of $Bi_5O_7NO_3$ in removal of MO dye from an aqueous solution. Experimental conditions: 20 mg L^{-1}, 1.0 g, solution pH and 298 ±1K.

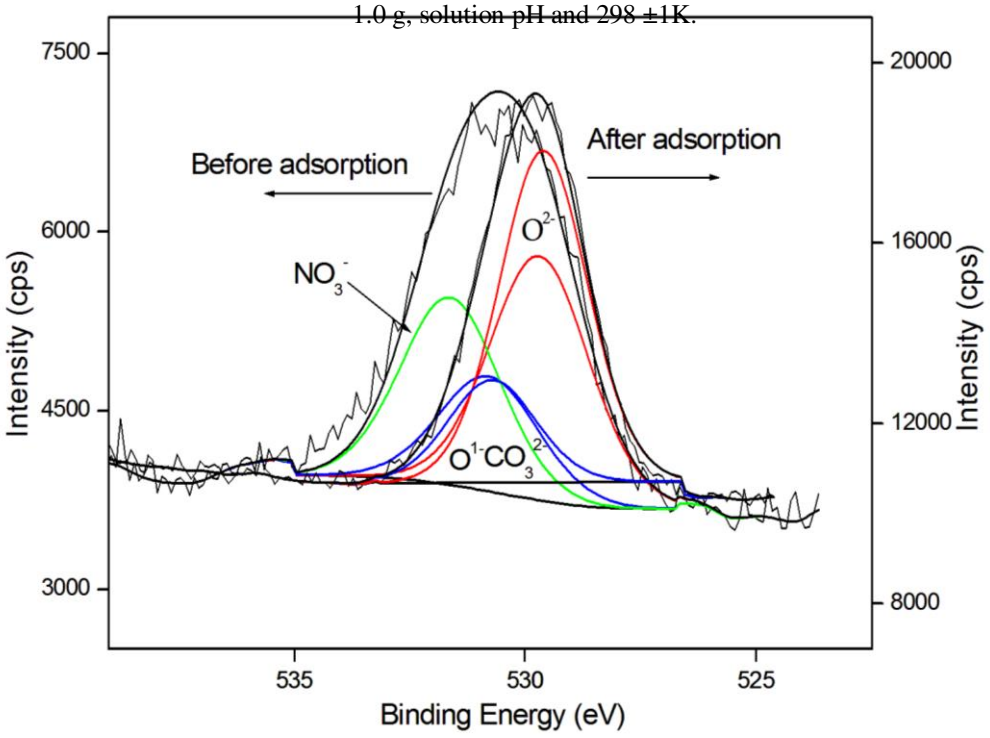

Figure 9: XPS spectra of O 1s core level region of $Bi_5O_7NO_3$ before and after MO dye adsorption.

Conclusion

A chemical precipitation method was successfully used to synthesize the orthorhombic $Bi_5O_7NO_3$ in this study. The binding energies were in close agreement with the results obtained for Bi_2O_3, suggesting the three oxidation states of bismuth atoms in $Bi_5O_7NO_3$. The higher surface basicity of $Bi_5O_7NO_3$ might correlate with its sorption efficiency in a wide range of pH. The sample had a good adsorption performance in removing the methyl orange dye from the aqueous solution, hence, it exhibited a great potential as a new adsorbent. The adsorption mechanism revealed that $Bi_5O_7NO_3$ can be considered as an alternative anion exchanger for azo dye removal.

Acknowledgment

The authors are grateful to Taiz University, Yemen, for their financial support of Eshraq's scholarship.

References

1. Kodama H. *J Solid State Chem.* 1994, **112,** 27.
2. Ziegler p, Strobele M, Meyer H-J. *Z Kristallogr* 2004, **219,** 91.
3. Henry N, Mentre O, Abraham F, Maclean Ej, Roussel P. *J Solid State Chem.* 2006, **179,** 3087.
4. Kodama H. *Bull Chem. Soc. JPN* 1994, **67,** 1788.
5. Rivera-Utrilla J, Bautista-Toledo I, Ferro-Garcı´a M, Moreno-Castilla C. *J. Chem. Technol. Biotechnol.* 2001, **76,** 1209.
6. Fernandes FM, Araújo R, Proença MF, Silva CJR, Paiva MC. *J. Nanosci. Nanotechnol.* 2007, **7,** 3514.
7. Desikusumastuti A, T.Staudt, gronbeck H, J.Libuda. *J. Catal.* 2008, **255,** 127.
8. Ruiz ML, Lick ID, Ponzi MI, Castellon ER, Jimenez-Lopez A, Ponzi EN. *Thermochim. Acta* 2010, **499,** 21.
9. Reddy KRk, Suneetha. P, Karigar. CS, Manjunath NH, Mahendra KN. *J. Chil. Chem. Soc.* 2008, **53,** 1653.
10. Irmawati R, Nasriah MNN, Taufiq-Yap YH, Hamid SBA. *Catal. Today* 2004, **93-95,** 701.
11. Fruth V, Popa M, Berger D, Ionica CM, Jitianu M. *J. Europ. Ceramic Soc.* 2004, **24,** 5.
12. Kumada N, Kinomura N. *J. Solid State Chem.* 1995, **116,** 281.
13. Jing-jing X, Min-dong C, De-gang F. *Trans. Nonferrous Met. Soc. China* 2011, **21,** 340.
14. Wildberger MD, Maciejewski M, Grunwaldt J-D, Tamas Mallat AB. *Appl. Catal. A* 1999, **179,** 189.
15. Dai Y, Wang Y, Yao J, Wang Q, Liu L, Chu W *et al. Catal. Lett.* 2008, **123,** 307.
16. Watkins RS, Lee AF, Wilson K. *Green Chem.* 2004, **6,** 335.
17. Chen S, Zhang J, Zhang C, Yue Q, Li Y, Li C. *Desalination* 2010, **252,** 149.
18. Qing W, Guojun j, Hongpeng L, Jingru B, Shaohua L. *Oil Shale* 2010, **27,** 135.